Determination of the Specifications of an Enhanced Upper Mass of the aPLI and Evaluation of the Functional Performance of the First Prototype

Mehrdad Asadi, James French, Yukou Takahashi

Abstract The current aPLI is not facilitated to measure pelvic injury metrics while the EEVC upper legform impactor has failed to accurately represent the pelvic loads and kinematics in car-to-pedestrian impacts. The current study aimed to develop the specifications of a functioning prototype for a modified upper mass of the aPLI and experimentally validate its function of pedestrian pelvic injury measurement. A reduced human body model with the struck-side lower limb and the pelvis was subjected to impact from three simplified car models representing a sedan and an SUV with low and high bonnet leading edge. The key design parameters of the simplified pelvis were identified by iteratively varying the components' specifications to develop a simplified pelvis model. The first prototype of the aPLI upper mass was then designed, manufactured and subjected to generic vehicle test rig impact testing. The test results showed that the prototype successfully achieved its goal to measure pelvis injury metrics. This was the first study to provide experimentally obtained technical evidence, showing that the enhancement of the capability of the upper mass attached to the aPLI lower limb allows pelvis injury measurements in a subsystem test for pedestrian safety.

Keywords Modified aPLI, pelvis injury, modified upper mass

I. INTRODUCTION

The advanced pedestrian legform impactor (aPLI) SBL-B was successfully launched in 2021, as the result of a project run by the aPLI task group under ISO TC22/SC36/WG5&WG6. The requirements for the aPLI were added to Euro NCAP 2023 protocol as well as other NCAP programme worldwide [1]. Despite its extended injury assessment capability to the thigh from the conventional legform covering the knee and the leg, aPLI still lacks capability to measure pelvic injury metrics. In a previous study, it was found that the EEVC upper legform impactor [2] was unable to represent the sustained loads and behavioural pelvis kinematics during a car-to-pedestrian impact appropriately [3]. Another study investigated the effect of the upper body and lower limb (LL) in pelvis injury measurements but not the sustained loads and injury mechanism [4]. Subsequently, the results of a study conducted by Japan Automobile Manufacturers Association (JAMA) and Japan Automobile Research Institute (JARI) were presented in which a new pedestrian pelvis impactor was evaluated to address pelvis injury and mechanisms [5]. Pelvis deflection [6], pubic symphysis (PS) were used as criteria for pubic rami fractures which is frequent in car-pedestrian accidents Sacroiliac joint (SIJ) forces was also selected as an additional injury criterion for sacroiliac joint fractures which occur less frequently, but can have serious consequences [7]. They also found that the pelvis injury measures were insensitive to non-struck side (NSS) LL geometry and it could be replaced with a concentrated mass attached to the NSS illum. Although those results gave sufficient confidence and credible evidence to suggest the feasibility of an updated upper mass (UM) for aPLI that can add to its capabilities to measure pelvis injury metrics, they only involved computational analyses without hardware testing. The current study was a continuation of the previous JAMA-JARI study to specify the key design parameters of a simplified pelvis model of a reduced human body model (HBM) that was validated against the baseline full-body HBM. The results were then used to design a functioning prototype of the aPLI modified UM and test it with the current aPLI LL in a subsystem test against the generic vehicle test rig (GVTR) developed by European Automobile Manufacturers Association (ACEA) [14].

II. METHODS

Computational Modelling

A multi-step parametric study was carried out to reach the specifications of a simplified pelvis model of an HBM. Due to limited Post-Mortem Human Subject (PMHS) data, the study relied on comparing impactor responses

M. Asadi (e-mail: Mehrdad.Asadi@cellbondimpactsolutions.com) is the Business Unit Manager for Cellbond Impact Solutions in Huntingdon, UK. J. French is the Head of Engineering at Encocam Ltd., Huntingdon, UK. Y. Takahashi is the chair of the Pedestrian Protection Experts Group of the Japan Automobile Manufacturers Association, Inc.

with reliable Human Body Models (HBMs). Although a brief summary of the study was given in [8], this paper provides a full description of the work. The HBM developed in a previous study [9] [10] [11] was used as the response baseline in this Work. This HBM was validated by the using the following data:

- Mid-shaft, distal third dynamic 3-point bending to failure for the femur, tibia and fibula
- Mid-shaft and distal third dynamic 3-point bending to failure for the thigh (femur with flesh)
- Mid-shaft, distal third dynamic 3-point bending to failure for the leg (tibia and fibula with flesh)
- Quasi-static and dynamic tension to failure for the knee ligaments (anterior and posterior bundles of ACL and PCL, LCL and MCL)
- Dynamic 4-point bending to failure for the knee joint
- Quasi-static compression and tension of the pubic symphysis
- Dynamic lateral compression of the pelvis (acetabulum loading, iliac loading)
- Trajectories in lateral collision at 40 km/h with a sedan and an SUV (Head, T1, T8 and pelvis)

The first step of current study aimed to generate a set of data using the full-body HBM impacted by three simplified car models (SCMs) representing an average sedan, an SUV with a low bonnet leading edge (BLE) and an SUV with a high BLE (hereafter referred to as Sedan, SUV-Low and SUV high, respectively) at 11.11 m/s (40 km/h) impact speed (Fig. 1). These data were used as the baseline responses, while the next steps are executed to reach a simplified pelvis model of the HBM using the same impact scenarios.

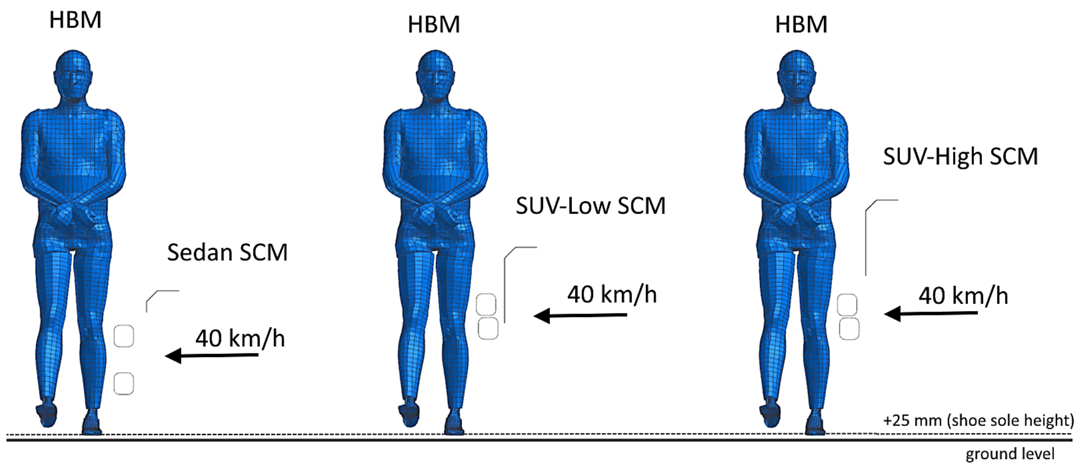

Fig. 1. Full-Body HBM subjected to Sedan, SUV-Low and SUV High SCM impacts at 11.1 m/s speed.

In the second step, the simplification process of the HBM was initiated. Results from a previous study [5] were used to reduce the HBM (reduced HBM) by removing the insensitive geometric attributes as shown in Fig. 23. The hip joint's degree of freedom (DoF) was also investigated in this step and the spherical joint was simplified the details can be seen in Fig. 27.

The third step focused on the inertial attributes of the NSS LL by optimising the position and magnitude of the concentrated mass (Fig. 25 in Appendix 1) that was introduced in a previous research work [5].

Based on the results of a sensitivity study, candidate materials were nominated for the simplified pelvis model of the reduced HBM in the fourth step. The list of initial materials and a comparison of the component mass is shown in TABLE II in Appendix 1. In this step, the candidate materials were assigned to the components individually and the suitable material was selected based on the best correlation with the baseline HBM responses generated in step one.

In the fifth step, the geometry of the insensitive parts of the struck side (SS) ilium was reduced and the NSS ilium was further simplified during individual processes as shown in Fig. 39 and Fig. 41 in Appendix 1.

The results from the steps 2-5 were then combined and formed the specifications of the simplified pelvis model of the reduced HBM. The reduced HBM was validated against the baseline HBM responses from step 1. The key design parameters of the simplified pelvis model were used to identify the specification of the first physical prototype of the modified UM of aPLI (hereafter called prototype-1).

A sensitivity study evaluated the effect of the variation in the geometry, stiffness and mass of the pelvis components on its injury metrics, when subjected to the SCM impacts [8]. To maintain the consistency with the previous studies [5] [6], pelvis deflection, pubic symphysis (PS) force and sacroiliac joint (SIJ) force were selected as injury metrics during the simulations (Fig. 2).

Pelvis deflection was measured by calculating the relative displacement between two nodal probes that were defined on the SS and NSS acetabulum. The forces in pubic symphysis and sacroiliac joints were measured using cross-section probes in each joint. The x-direction (direction of the SCM impacts) of the response forces for the sacroiliac joint and pubic symphysis were considered in this study.

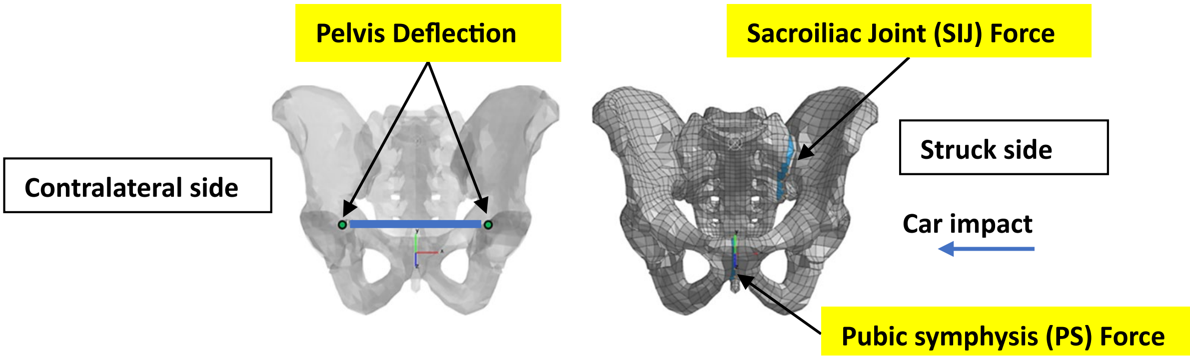

Fig. 2. Pelvis injury criteria used in this study (pelvis deflection, pubic symphysis and sacroiliac joint force).

The responses from each iteration were evaluated against the corresponding ones from the baseline HBM. The maximum values of the pelvic injury metrics were obtained from the reduced HBM simulations and the corresponding full-body HBM simulations (baseline responses). To analyse the correlation between the responses, an acceptable range of the coefficient of determination (R^2) of 0.5 and higher, and the range of the regression coefficient (gradient) of 0.8 to 1.2 were used as evaluation criteria [5] [12] [13].

Design, Manufacturing and Testing the Prototype-1

The specifications of the validated simplified pelvis of the reduced HBM were used as the baseline to design the prototype-1. The outcome of the mechanical design process was a prototype representation of the simplified pelvis of the reduced HBM. The results of the sensitivity study (TABLE I in Appendix 1) were also used to determine the allowable design freedom. Sensitive areas should not deviate from the FE model, however, areas that were found to be less sensitive (or insensitive) were open to design freedoms.

The reduced HBM lacked representation of the moment-angle response of the hip joint, while pelvic injury metrics were found to reasonably match those from the HBM. This suggested that the lack of the adduction bumper system should not have a significant impact on the validation of the functioning of the prototype-1's hardware as a subsystem impactor, capable of measuring pelvic injury metrics.

The prototype-1 hardware was fabricated and equipped with appropriate data acquisition systems (DAS) to measure the responses during the dynamic impact testing.

Prototype-1 testing

To evaluate the functionality of the prototype-1, it was assembled with the aPLI LL and mounted on a launching device and projected onto a stationary vehicle front-end substitute. A gravity sled (Fig. 3) was used to accelerate the prototype-1 with the aPLI LL (hereafter called prototype-1 assembly) to 11.1 m/s (40 km/h). The prototype-1 assembly was supported by a rigid frame that was guided toward the impact. The frame was stopped a distance before impact of the prototype-1 assembly with the GVTR, and the prototype-1 assembly was allowed to fly freely and unaidedly to impact with the GVTR. Due to the setup of the sled, the prototype-1 assembly could only be accelerated horizontally with no allowance for ballistic correction.

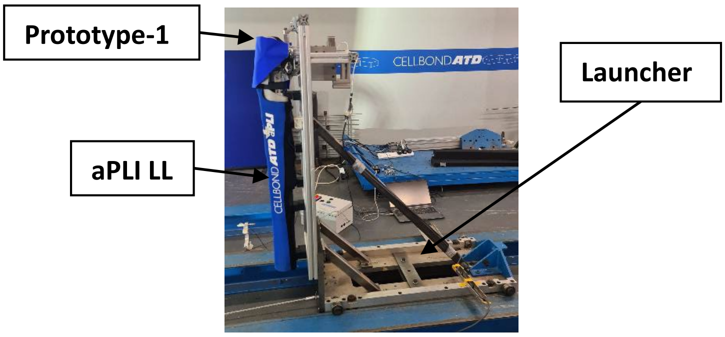

Fig. 3. Prototype-1 test setup.

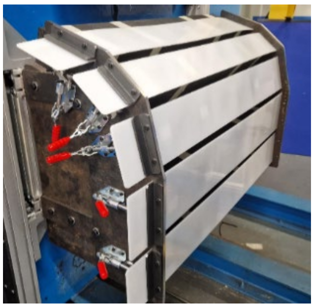

Fig. 4. GVTR SUV configuration was used as the evaluation tool for the prototype-1.

The height of the GVTR could be adjusted to achieve both SUV-high and SUV-low test setups. However, the SUV-high configuration of GVTR [14] was selected and manufactured as the car substitute (Fig. 4). The bumper system installed at the hip joint of the aPLI provides moment vs angle response of the hip joint, reducing the unrealistic femur bending moment to better align with HBM performance [15]. Due to the absence of the bumper system in the simplified pelvis model of the reduced HBM (and subsequent prototype-1), it was considered important to define test conditions such that the modified UM has the lowest influence of the hip joint adduction over the pelvic and aPLI LL response. Consistently with a previous study [16], two SUV BLE positions of 868 mm and 903 mm were assessed initially. However, 903 mm height was chosen for the physical test set up to further distribute the impact load between the UM and the upper part of the femur across the hip joint and minimise the influence of the hip joint rotation of the prototype-1 assembly during the impact test.

The prototype-1 assembly was positioned in accordance with the aPLI setup parameters, following the Euro NCAP test protocol [17], which define, at the point of impact, an offset from the ground level of 25 mm. According to the Euro NCAP protocol, the direction of impact at the point of first contact shall be in the horizontal plane with a tolerance of ±2°. Due to the limitations, this criterion could not be achieved since the free flight distance of 850 mm and a calculated drop in height of 29 mm. The release velocity was measured just before the sled started decelerating.

III. RESULTS

Computational Modelling Results

TABLE I in Appendix 1 provides a summary of the sensitivity study that evaluated the pelvis injury metrics against the variation of the HBM pelvis component attributes. These results were used during the iterative steps in this work. The combination of the findings from five steps resulted in the specifications of the simplified pelvis components of the reduced HBM. The iterative steps to reach the final model using a parametric study approach have been detailed in Appendix 1. The final model for the reduced HBM contained the simplified hip joint model, selected materials for the pelvis components and the simplified geometries for the SS and NSS ilium parts. the simplified SS and NSS ilium were combined to form a reduced HBM with the simplified pelvis model that offers design parameters of a functioning prototype for a modified UM (Fig. 5).

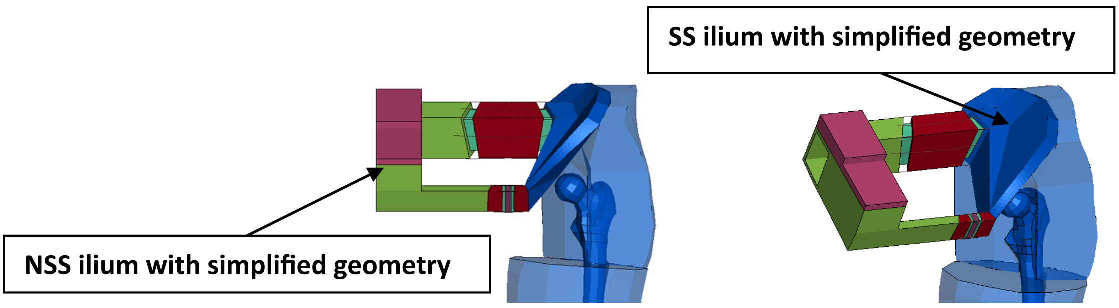

Fig. 5. The final simplified pelvis model of the reduced HBM.

Hereafter, to illustrate the findings in this study (including the ones in Appendix 1), colour coding will be used as shown in Fig. 6. The colour of the circle indicates the variables while, the coulour of the enclosure box shows the type of the SCM in the simulation iteration.

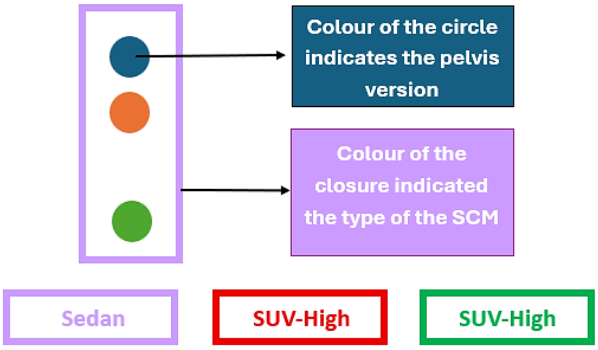

Fig. 6. Colour-coding used to illustrate the results.

Fig. 7 shows the pelvis response in the reduced HBM when the model is first updated with the selected materials (TABLE II in Appendix 1) for the components and then additionally with the simplified geometries of the SS and NSS ilium. The sacroiliac joint force showed the largest difference in SUV-High impact when both materials and geometries were updated. The results for the sacroiliac joint force correlated well for the Sedan and SUV-Low SCM responses, however, there was an increase in the SUV-High SCM response. Nonetheless, the slope of the trendlines stayed within the assumed limits and the coefficients of the determination stayed well above 0.5 value.

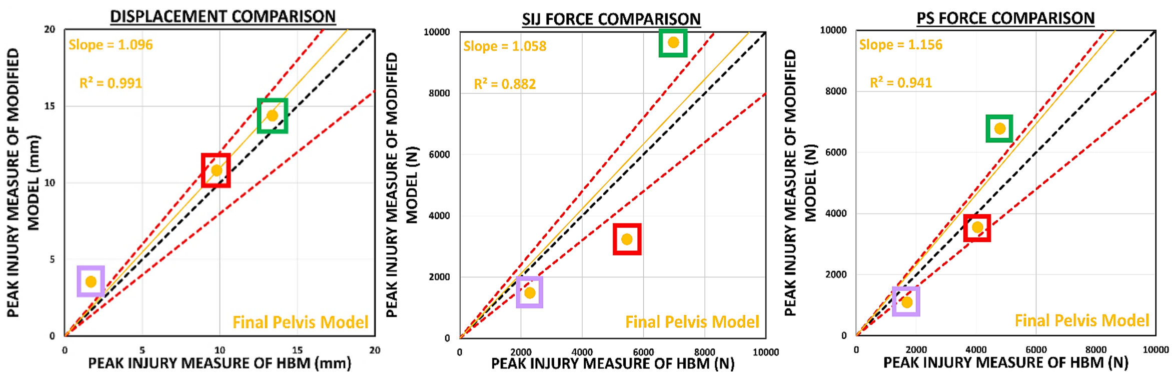

Fig. 7. Pelvis responses of the final simplified pelvis model of the reduced HBM compared with the baseline HBM responses.

Designing the Components of the Prototype-1

With the design parameters for the prototype-1 specified in the computational modelling stage, these specifications were employed to design the prototype-1 components in the following steps during the design phase, where X, Y and Z axis are defined as posterior to anterior, left to right and superior to inferior, relative to a pedestrian body, respectively.

SS Ilium Design

The mechanical design of the SS ilium highlighted some significant areas for review, particularly around the aPLI LL hip joint. The SS ilium needed modification to allow for integration with the aPLI LL. The two main areas for review were the hip joint location and the volume of the top of the femur as the relative volume of the top of the femur of the aPLI LL was significantly larger than the HBM LL. As the acetabulum forming the hip joint is located in the lower part of the ilium, this had consequences for the lower sections of the SS ilium. During the mechanical design, the stiffness of the upper section of the SS ilium was not modified, however, due to the mechanical attachment of the SS sacroiliac joint, material needed to be added to parts of the upper sections of the SS ilium. An additional modification to the lower sections of the SS ilium was required to allow for mechanical fasteners to be added for attachment of the aPLI hip joint. Fig. 8 shows the final design of the SS ilium in prototype-1. A comparison between the physical properties of the SS ilium in the simplified pelvis model of the reduced HBM and prototype-1 is given in TABLE IV and TABLE V in Appendix 2.

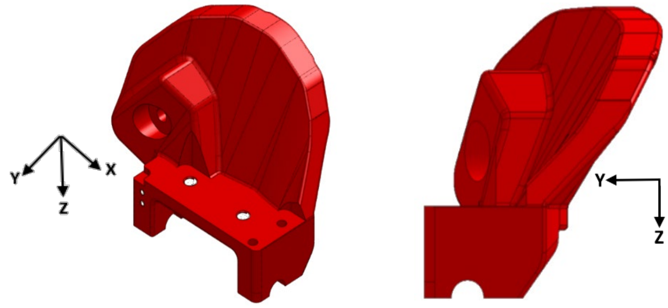

Fig. 8. Final design of the prototype-1 SS ilium

NSS Ilium Design

Results from TABLE I in Appendix 1 suggested that pelvic injury metrics were sensitive to the mass and CoG location of the NSS ilium, whilst its geometry and stiffness are insensitive parameters. Furthermore, pelvic injury responses were also insensitive to the stiffness of the NSS sacroiliac joint. Therefore, the NSS sacroiliac joint could be replaced with a rigid connective piece with the same mass and CoG. In addition, the sacrum which was represented by a volume of material with mass and CoG in the simplified pelvis model of the reduced HBM, could also be rigidly attached to the NSS ilium and the NSS sacroiliac joint. This meant that the NSS ilium, NSS sacroiliac joint and sacrum could be represented by one single rigid component, hereafter referred as the NSS assembly in this paper. This allowed practical improvements such as a reduced part count and improved assembly repeatability through reduced tolerance accumulation and assembly error, without adverse effects on the pelvis injury measurements. The NSS assembly was chosen for the location for the data acquisition system DAS installation due to its insensitivity (and therefore design freedom) with respect to its geometry and overall shape, provided that the total mass and CoG location of the combined components were maintained. The NSS assembly also offers relative protection to the DAS from impacts during tests or secondary or accidental impacts. Fig. 9 shows the details of the NSS assembly.

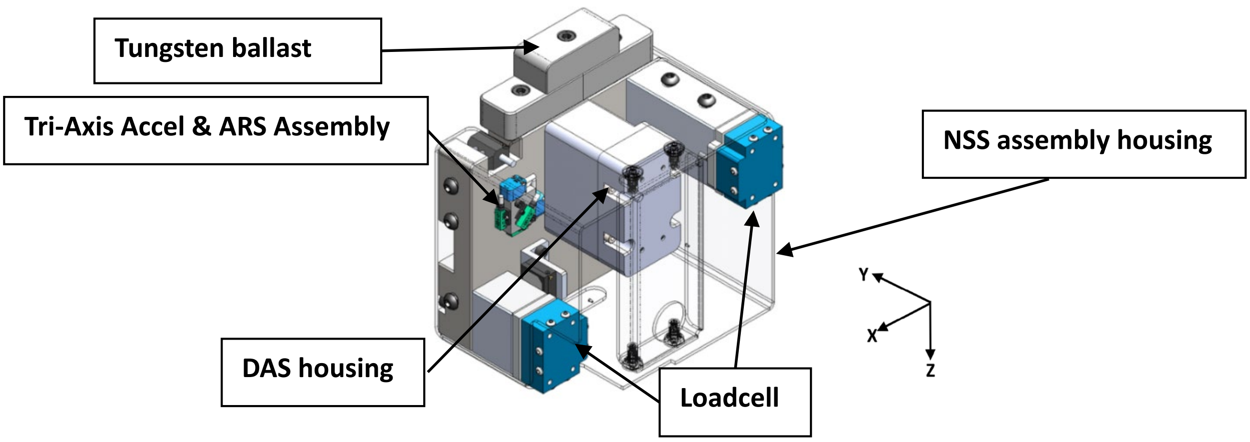

Fig. 9. NSS assembly of the modified UM

A comparison between the physical properties of the combination of the sacrum, sacroiliac joint and NSS ilium in the simplified pelvis model and prototype-1 is given in TABLE VI and TABLE VII in Appendix A.

Hip Flesh Design

Sensitivity study results in TABLE I in Appendix 1 showed that the pelvis injury metrics were sensitive to the stiffness of the SS hip flesh, while its geometry was an insensitive parameter. However, to maintain the contact profile of the simplified HBM, the SS hip flesh external geometry was based on the hip flesh of this model. A polyurethane (PU) material was selected for prototype-1 as used in the aPLI flesh components. Although flesh components are not directly used for injury assessment, they do affect the impactor's response. Therefore, instead of comparing properties at the component level, injury metrics that account for the influence of flesh components were evaluated during impact. During the design of the SS ilium, it was shown that the attachment of the aPLI LL to the prototype-1 UM requires modification to the SS ilium. The removal of the curved femur top in aPLI was essential to allow the attachment of the prototype-1 UM to the aPLI LL, as clearly illustrated by the schematic of the prototype-1 SS ilium superimposed on the aPLI LL with the femur top in Fig. 10. Given that the SS hip flesh geometry was proven to be insensitive, this was considered an acceptable change. Fig. 11 shows the final design of the SS hip flesh in prototype-1. A comparison between the physical properties of the SS hip flesh in the simplified HBM and prototype-1 is given in TABLE VIII and TABLE IX in Appendix 2.

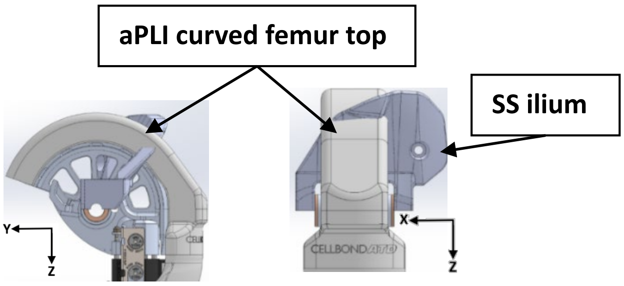

Fig. 10. Schematic of SS ilium of prototype-1 superimposed onto the aPLI LL with curved femur top.

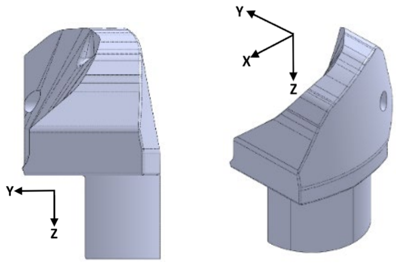

Fig. 11. Prototype-1 SS hip flesh

Compliant Joint Design

The SS sacroiliac joint and pubic symphysis were modelled as compliant joints covered by ligaments in the simplified pelvis model. As these ligaments offer no compressive properties, the compliant joints are allowed to compress, but extension is limited due to the tensile properties of the ligaments. In addition, when bending is applied to these joints, the compressive force is generated on the joint surfaces, due to the tensile force created by the ligaments on the stretched side of the joint. Relative to pure compression, this mechanism increases the compressive force and thus risk of fracture at the joint when combined compression and bending is applied to the joint. Pelvic injury metrics have been shown to be sensitive to the SS sacroiliac joint and pubic symphysis stiffness but not their geometries (TABLE I in Appendix 1). Therefore, a simplified mechanical representation, including the integration of the ligaments, was developed as part of prototype-1. The compliant element was designed in such a way that it can be easily removed from the prototype-1 structure (Fig. 12).

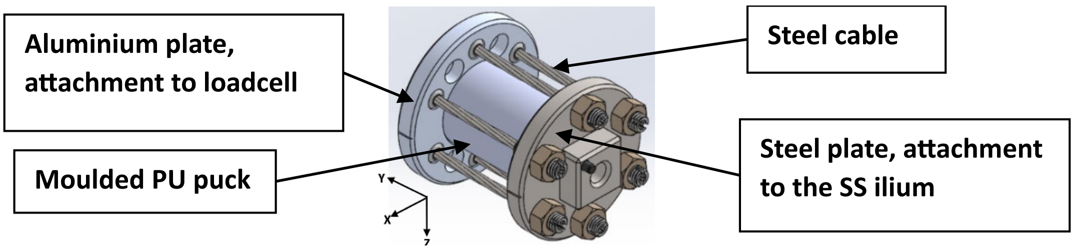

Fig. 12. Construction of the compliant joints for prototype-1.

The compliant joints consisted of two metal plates with a polyurethane (PU) puck between them. The PU puck provided the compressive properties of the compliant joint, with the two metal plates creating the loading surfaces to the puck. Six wire ropes, with a diameter of 3 mm, equally spaced around the circumference of the metal plates were used (Fig. 12). The ends of each wire rope were fixed to their respective plates, with the design intent being for the cables to buckle during compression loads and minimise the effect on overall compliant joint compression. To further simplify the physical aspects, both the SS sacroiliac joint and pubic symphysis used compliant joints of the same geometry, though made from dissimilar materials to represent the different stiffness requirements. A comparison of geometric attributes of the compliant joint between the simplified pelvis model and prototype-1 is given in TABLE X in Appendix 2.

Instrumentation and DAS

A review of existing ATD instrumentation was undertaken, with the pubic load cell [18] from the WorldSID and Q10 dummies was identified as most suitable for the SS sacroiliac joint and pubic symphysis locations. This was based on size limitations, loading capacity and the requirement to measure only one axis.

The attachment of the aPLI LL at the hip joint did not allow the displacement measurement location employed in the simplified pelvis model to be used. Therefore, two string potentiometers, equally shifted in the x-direction whilst maintaining the z-location relative to the measurement in the simplified pelvis model, were assigned in the design (Fig. 13). A mean value that gave a representation of the central displacement was calculated by averaging the displacement values from the potentiometers 1 and 2.

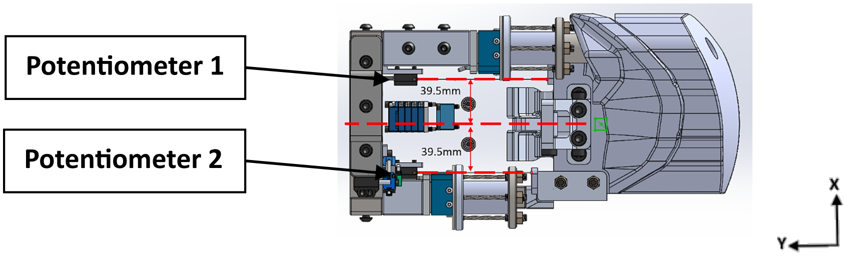

Fig. 13. Displacement measurement locations (top view of the modified UM)

The existing accelerometers and angular rate sensors (ARS) from the aPLI UM were relocated to the NSS assembly to monitor the prototype-1 UM during impact.

Prototype-1 assembly

Fig. 14 shows the CAD assembly of the modified UM for prototype-1. The prototype-1 components were manufactured and the modified UM assembly was fabricated based on the specifications discussed previously. Fig. 14 shows the images from the assembled prototype-1.

To allow dynamic testing of the prototype-1 hardware, consideration was needed to ensure that it was appropriately supported during the acceleration phase of the launch and subsequent release from the launcher device. The prototype-1 hanging mechanism can be seen in Fig. 15.

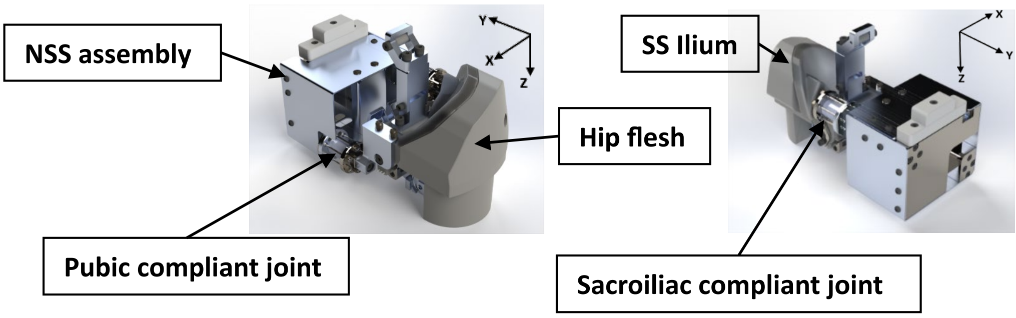

Fig. 14. CAD assembly of prototype-1.

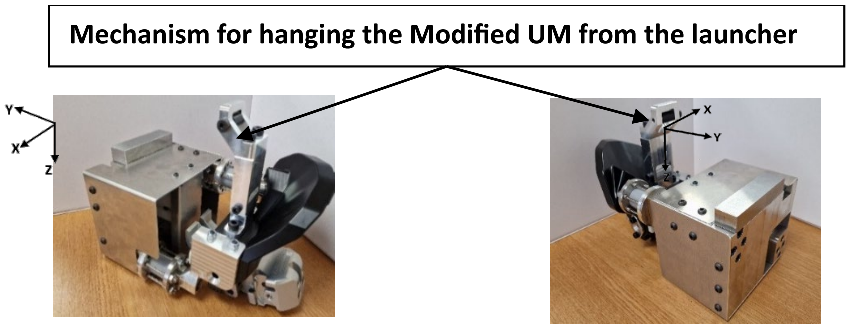

Fig. 15. Assembly of prototype-1 (flesh component is not attached)

Experimental Results

The GVTR SUV impact test was carried out and the prototype-1 responses were recorded successfully. Fig. 16 shows a visual review of the prototype-1 assembly during the impact with images showing free flight, mid-impact and rebound. The kinematics show that the prototype-1 assembly UM remained stable during free flight and that the LL does not appear to have been affected by the introduction of the modified UM. For this test the impact velocity was recorded at 11.16 m/s.

Fig. 16. Free flight, mid-impact and rebound kinematics of prototype-1 assembly in GVTR SUV impact test.

The results for the sacroiliac joint and pubic symphysis forces and the pelvis deflection are plotted during the first 40 ms of the impact against the sequential images from the experiment in Fig. 17. A close inspection of the compliant joints after the test indicated that some of the steel cable ligaments had experienced permanent deformation. Fig. 18 shows the details of the deformed steel cables. This highlighted the importance of further study of the joint mechanism during the next phases of the research.

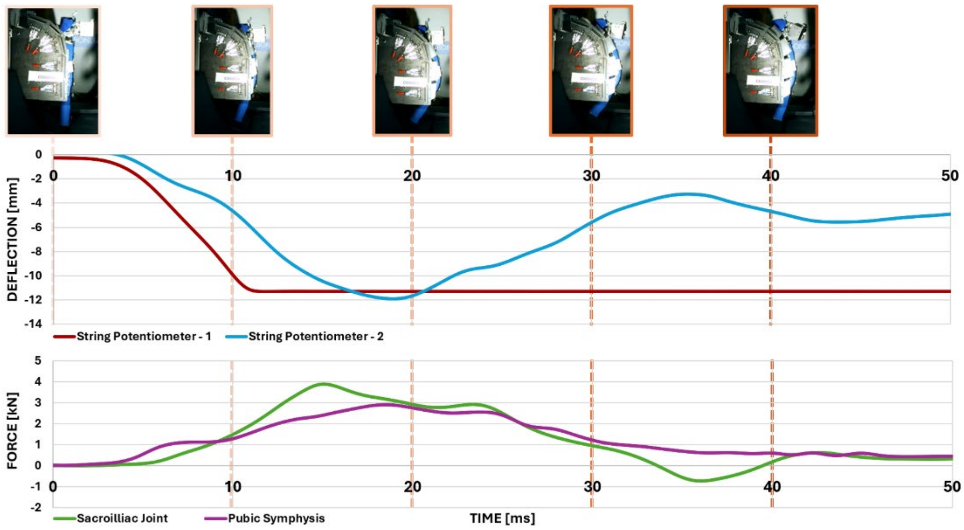

Fig. 17. Time history plots of prototype-1 pelvis force and displacement in GVTR SUV impact test.

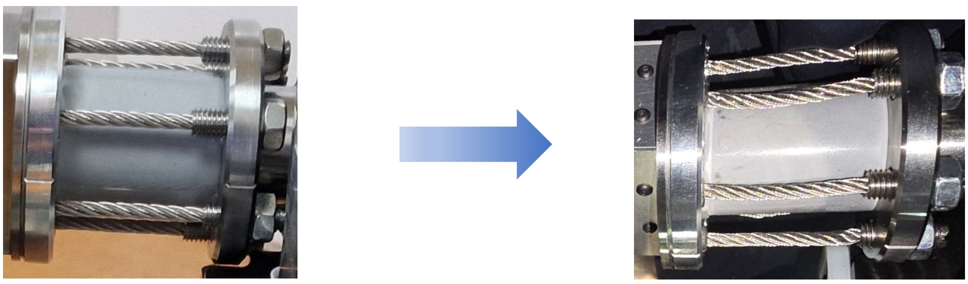

Before impact After impact

Fig. 18. Permanent deformation of the steel cable ligaments.

Results from the pelvic deflection data indicated an apparent anomaly from one of the string potentiometers, as shown in Fig. 19. This anomaly was caused by the incorrect assembly of one of the potentiometers and resulted in insufficient string retraction length before the sensors recoil stop was contacted. Due to this lack of data, it was not possible to calculate a meaningful central displacement as described previously.

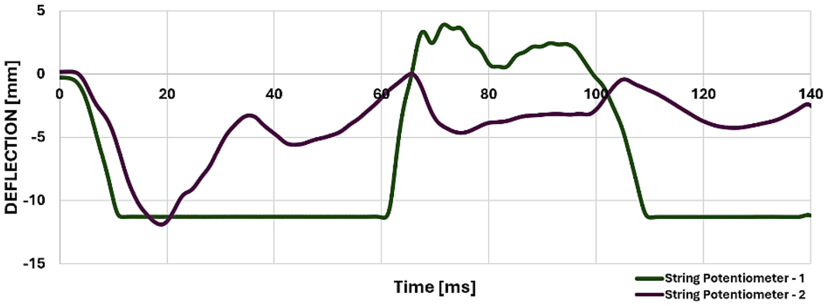

Fig. 19. Time history plots of prototype-1 pelvis displacement in GVTR SUV impact test.

IV. DISCUSSIONS

In this study, a physical prototype of the aPLI modified UM was developed based on the characteristics gathered in a parametric CAE study that resulted in a reduced HBM that contained the pelvis that was manufacturable and constructed using materials that are commonly implemented in ATDs. The reduced HBM provided the fundamental design requirements, constraints and physical specifications for the prototype-1 of the modified UM.

Despite its simplicity, the model offered a good correlation when the peak values of the pelvis injury criteria were compared with those from the HBM (pelvis deflection: R^2 = 0.991, sacroiliac joint force R^2 = 0.882, and pubic symphysis force: R^2 = 0.941) when subjected to the Sedan, SUV-Low and SUV-High SCM impacts. The pelvis displacement measured by the reduced HBM was higher than the ones from the baseline HBM response in the SUV-Low and SUV-High impacts. This could be due to the simplified geometry of the SS ilium, particularly in the SUV-High SCM impact that the load is directly applied to the SS ilium of the pelvis. The sacroiliac and pubic symphysis forces in the simplified pelvis model of the reduced HBM were measured lower in the Sedan and SUV-Low SCM impacts, whereas they were measured higher in the SUV-High SCM impact, compared to the full-body HBM results. This could be due to the differences in the kinematics of the pelvis between the reduced HBM and the full-body HBM, specifically in the rotation about the y-axis that is dominated by the NSS ilium (Fig. 20). While evaluating the results, to keep the consistency with the previous study [5], a target range of 0.8-1.2 was assigned to the slopes value of the regression line. These were higher than 1.0 for all the pelvis injury metrics, however, it still remained within the limit of the targeted range (Fig. 7).

Time (s)	0.000		0.015		0.030	
	Reduced HBM	HBM	Reduced HBM	HBM	Reduced HBM	HBM

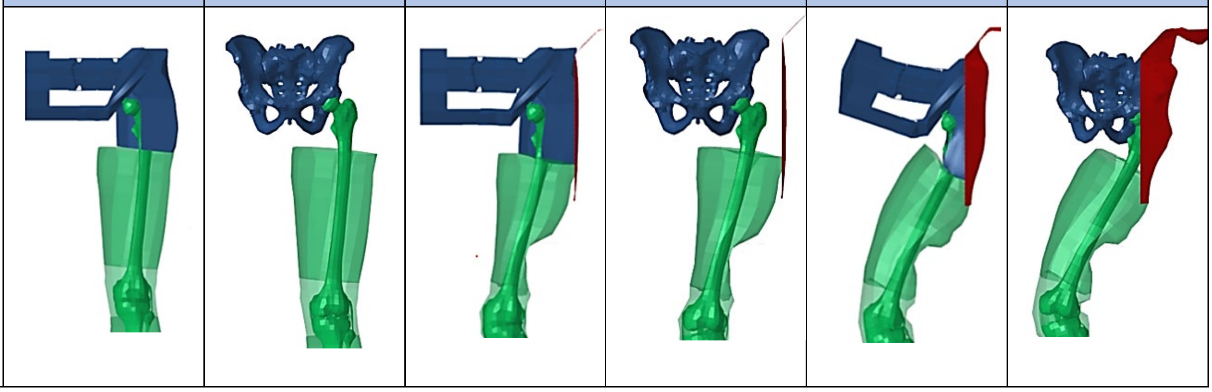

Fig. 20. Comparison of pelvis kinematics between full-body HBM and reduced HBM in SUV-High SCM impact. Higher rotation can be observed in the pelvic area in the reduced HBM.

The differences in pelvis kinematics between the reduced HBM and the full-body HBM can be related to the assumptions adopted during the simplifying process. For instance, the NSS LL was substituted with a concentrated mass rigidly attached to the contralateral hip joint to imitate the inertial effect of the limb on the pelvis response. The mass and moment of inertia provided by the specifications determined by this study may not have been an optimum solution. Therefore, further study is required to optimise compensation for the lack of NSS LL.

The design of the prototype-1 UM was based on the key parameters given by the reduced HBM. When subjected to the GVTR SUV impact test, the prototype-1 UM successfully generated the output data for pelvis deflection, sacroiliac joint force and pubic symphysis force through the assigned DAS. Despite malfunctioning one of the string potentiometers to measure the displacement, the initial results indicated that the prototype-1 UM could produce force and deflection measurements during a dynamic impact when assembled with the aPLI LL. The choice of GVTR SUV proved to be effective to minimise the rotation of the prototype-1 during the impact, even in the absence of the adduction bumper system in the prototype-1 assembly. The prototype-1 UM did not present major rotation during free flight and the aPLI LL did not seem to have been influenced by the adaption of the modified UM.

The permanent deformation of the steel cable ligaments in Fig. 18 could be due to the compression of the compliant joints during the impact, with the cable unexpectedly resisting compression. In the current design, the force transferred through the cables would be transferred to the load cell, resulting in an inaccurate output to address fracture at the joint surface. This also indicated that the compliant joint had deformed larger than the initial expectations. The specifications, performance and design of those compliant joints require further study.

V. LIMITATIONS

As both the reduced HBM and the prototype-1 assembly hardware did not include the adduction bumper system, the evaluation had been limited to the test conditions most favourable to minimal UM rotation. To enable testing of the different vehicle heights, the bumper system, as used in the aPLI, will need to be incorporated into the FE model and future prototypes. Only Sedan, SUV-Low and SUV-High SCMs and GVTR SUV configuration were used to represent car front-end structures during this study. Any future optimisation would require incorporation of larger number of load cases not only to understand the behaviour of the modified UM better, but also to have a deeper insight into the influence of the modified UM specifications on the pelvis and aPLI LL responses to derive optimised design parameters for the modified UM.

During the development of prototype-1, certain assumptions were made, resulting in differences between the specifications of the modified pelvis FE model and the prototype-1 UM. While these differences did not impact the validation of the functionality of the prototype-1 UM, the resultant variation in response remains unknown at this time. Further optimisation is needed to improve the structural response of the compliant joints as they play key roles in transferring the loads between the pelvis components.

VI. CONCLUSION

The pelvis of the reduced HBM capable of reproducing pelvic injury metrics in car-pedestrian impacts was simplified for its material and geometric characteristics within the acceptance tolerances to derive key design parameters of the modified UM of aPLI. The information obtained was used to design and fabricate the prototype-1 UM of aPLI, and the prototype-1 UM hardware was used to run a dynamic subsystem test against the GVTR representing an SUV. The test results successfully demonstrated the functional ability to measure pelvis injury metrics in a simulated car-pedestrian impact and proved that the modified upper mass can add pelvis injury measurement capabilities to the aPLI impactor.

VII. REFERENCES

[1] Stielau K and Blauth D., “Advanced Pedestrian Legform Impactor (aPLI),” in 16th Inetrnational LS-DYNA Users Conference, 2020.

[2] EEVC Working Group 17, " Improved test methods to evaluate pedestrian protection afforded by passenger cars," EEVC, 2002.

[3] Takahashi Y, Suzuki S, Ikeda M and Gunji Y, "Investigation on pedestrian pelvis loading mechanisms using finite element simulations," in IRCOBI, Hanover, 2010.

[4] Gunji Y, Okamoto M and Takahashi Y., "Examination of human body mass influence on pedestrian pelvis injury prediction using a human FE mode," in IRCOBI, Dublin, 2012.

[5] Isshiki T, Higuchi Y, Kato R, Antona M J, Konosu A, Takahashi Y., "Development of a Pedestrian Pelvis Impactor CAE Model with Potential to Address Pelvis Injury Loads and Injury Mechanisms," in IRCOBI Conference 2019, Florence, 2019.

[6] Gunji Y, Okamoto M and Takahashi Y., "Development of a pedestrian pelvis injury index using a human FE Model - a further study," in Proceedings of JSAE Spring Conference, 2011, Yokohama, Japan, 2011.

[7] Akiyama A, Okamoto M and Takahashi Y., "Estimation of injury measures for a pedestrian dummy pelvis," in Proceedings of JSAE Spring Conference, Yokohama, Japan, 2009.

[8] Asadi M, Bell C and Takahashi Y., "Optimisation of a New Pedestrian Pelvis Impactor," IRCOBI conference , Sweden, 2024.

[9] Takahashi Y, Kikuchi Y, Mori F and Konosu A, "Advanced FE lower limb model for pedestrian," in 18th ESV Conference, Paper number 218, 2003.

[10] Kikuchi, Y., Takahashi, Y., and Mori, F., "Development of a finite element model for a pedestrian pelvis and lower limb," in SAE 2006 World Congress & Exhibition, 2006.

[11] Kikuchi Y, Takahashi Y, and Mori F., "Full-scale validation of a human FE model for the pelvis and lower limb of a pedestrian," SAE Technical Paper, 2008, 01-1243.

[12] Isshiki T, Konosu A, and Takahashi Y., "Development and evaluation of the advanced pedestrian legform impactor prototype which can be applicable to all types of vehicles regardless of bumper height - Part 1: finite element model.," in Proceedings of IRCOBI Conference, Malaga, Spain., 2016.

[13] Teresiński G and MadroR., "Pelvis and hip joint injuries as a reconstructive factors in car-to-pedestrian accidents," Forensic Science International, vol. 124, no. 1, pp. 68-73, 2001.

[14] Feist F, Sharma N, Klug C, Roth F, Dornbusch F, Schinke S, Besch A., "GVTR: A Generic Vehicle Test Rig Representative Of The Contemporary European Vehicle Fleet," in The 26th International ESV Technical Conference, Eindhoven, Netherlands, 2019.

[15] ISO, Road vehicles — Design and performance specifications for advanced Pedestrian Legform Impactor (aPLI), ISO/TS 20458:2023, 2023.

[16] Konosu A, Isshiki T, Antona J, Higuchi Y, Winter D, Takahashi Y., "Biofidelity Improvement of Advanced Pedestrian Legform Impactor in Rebound Phase," in Proceeding of IRCOBI conference, 2020.

[17] EuroNCAP, "Pedestrian Tesing Protocol," European New Car Testing Programme, 2017.

[18] "Uniaxial Pubic Load Cell - Type M50241A Technical Data Sheet," Kistler Group, 2015.

[19] UN Regulation No 127, "Uniform provisions concerning the approval of motor vehicles with regard to their pedestrian safety performance [2020/638]," 2020.

APPENDIX 1: DETAILS OF COMPUTATIONAL ITERATIONS TO REACH THE SPECIFICATIONS OF THE SIMPLIFIED PELVIS OF THE REDUCED HBM

This appendix explains the details of the process that was employed in this research to reach the specifications of the simplified pelvis model of the reduced HBM in a multi-step manner. TABLE I shows the summary of the sensitivity study that has been used during the steps of the current study.

TABLE I
SENSITIVITY STUDY OF THE HBM PELVIS COMPONENTS. THIS TABLE SHOWS IF THE PELVIS INJURY METRICS WERE INFLUENCED DUE TO THE VARIATION OF THE ATTRIBUTES IN EACH COMPONENT.
P.D. : pelvis deflection, P.F. : pubic symphysis force, SI F. : sacroiliac force

Table Legend	Geometry			Stiffness			Mass		
Sensitive (red) / Insensitive (green)	P.D.	P.F.	SI F.	P.D.	P.F.	SI F.	P.D.	P.F.	SI F.
SS Soft Tissue	Insensitive	Insensitive	Insensitive	Sensitive	Sensitive	Insensitive	Insensitive	Insensitive	Insensitive
NSS Iliac	Insensitive	Insensitive	Insensitive	Sensitive	Insensitive	Insensitive	Sensitive	Insensitive	Insensitive
SS Iliac	Sensitive	Sensitive	Sensitive	Sensitive	Insensitive	Insensitive	Insensitive	Insensitive	Insensitive
Sacrum	Insensitive	Insensitive	Insensitive	Insensitive	Insensitive	Insensitive	Insensitive	Insensitive	Insensitive
SS SI Joint	Insensitive	Insensitive	Insensitive	Insensitive	Insensitive	Sensitive			
NSS SI Joint	Insensitive	Insensitive	Insensitive	Insensitive	Insensitive	Insensitive			
Pubic Symphysis	Insensitive	Insensitive	Insensitive	Sensitive	Insensitive	Insensitive			

Step 1: Creation of the Baseline Response Data Using a Full-Body HBM

To generate the baseline data, three car-to-pedestrian impacts at 11.1 m/s (40 km/h) were modelled. A validated 50th percentile male HBM [11] was used and the SCMs represented the front-end of a sedan (Sedan), a SUV with a low bonnet leading edge (SUV-Low) and a SUV with a high bonnet leading edge (SUV-High) [5].

The reason for selecting these specific SCMs was to assess different impact conditions over the pelvis and the lower limb of the HBM. The three SCM-HBM impact scenarios can be seen in Fig. 1.

The SCMs were arranged to impact the HBM in the upright (standing) posture, assuming the thickness of the sole of the shoe of 25 mm, as specified in UN regulations [19]. Gravitational acceleration (g = 9.81 m/s^2) was introduced in the model. Coefficient of friction between the HBM and the ground was set at 0.4, while it was set at 0.3 between the HBM and SCMs. Fig. 21 shows the HBM response when the HBM was subjected to impact against the Sedan, SUV-Low and SUV-High SCM. These responses were used as the baseline information to evaluate the responses from the parametric study of the pelvis FE models.

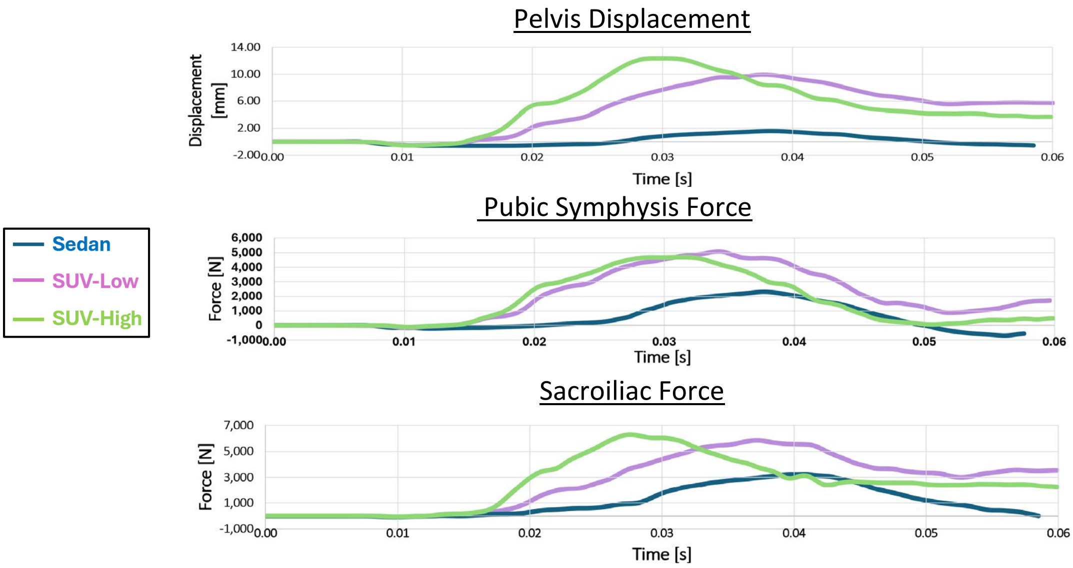

Fig. 21. Baseline HBM response to Sedan, SUV-Low and SUV-high impacts.

Step 2: Initial Simplification of the Full-Body HBM

Creating the Reduced HBM

The results from a previous study showed that the pelvis injury metrics were insensitive to the geometric and inertial property of the upper body in the HBM and it was an ineffective factor until the pelvic injury metrics reach their peak [5]. They also showed that the pelvis injury metrics were not sensitive to the geometry of the NSS LL, and the inertial property of the NSS LL can be represented by a concentrated mass of 3.87 kg on the NSS acetabulum. The mass and location used to represent pelvic injury metrics were determined empirically since due to the complex and varying kinematics of the contralateral side, it is challenging to model it with a simplified structure for consistent impact testing. The current study took these findings and recreated the reduced HBM by removing the upper body and the NSS LL from the HBM and assigning a nodal mass to the NSS acetabulum as shown in Fig. 22.

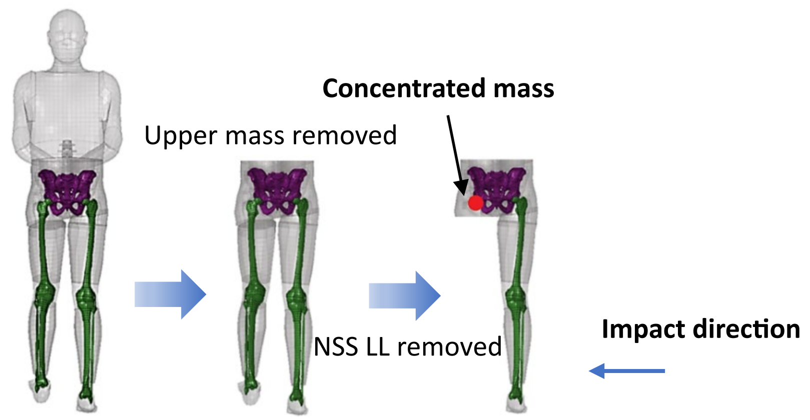

Fig. 22. Simplification process of the full-body HBM.

Simplifying the Pelvis Geometry

After creating the reduced HBM, the geometry of the SS and NSS ilium and the sacrum were further simplified. The results of the sensitivity study summarised in TABLE I shows that the pelvis injury measures are sensitive to the geometry of the SS ilium, while they are insensitive to the geometry of the NSS ilium and sacrum [20]. Therefore, the geometry simplification process of the SS ilium aimed to maintain a close biofidelic geometry profile of this component. The results in TABLE I show that the pelvis injury measures are insensitive to the sacrum's geometry, therefore, a simple profile was selected to the sacrum. The initial geometry of the NSS ilium was kept the same as the SS ilium at this stage. Since the two nodal probes at the acetabulum were used to measure the pelvis defection as an injury measurement, these locations were kept unchanged at the SS and NSS acetabulum. The details are shown in Fig. 23. The isolated geometry for the simplified pelvis FE model can be seen in Fig. 24.

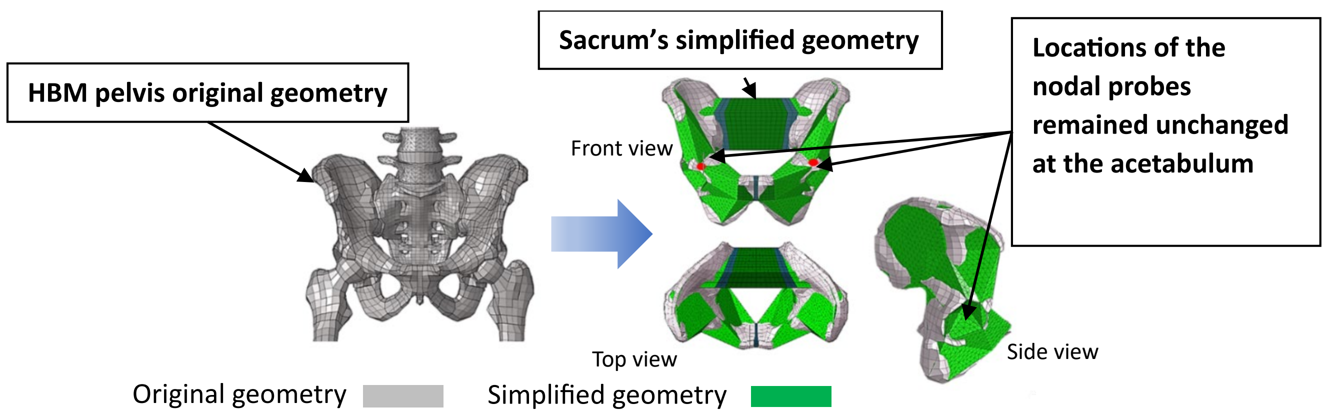

Fig. 23. Simplification of the geometry of the HBM Pelvis.

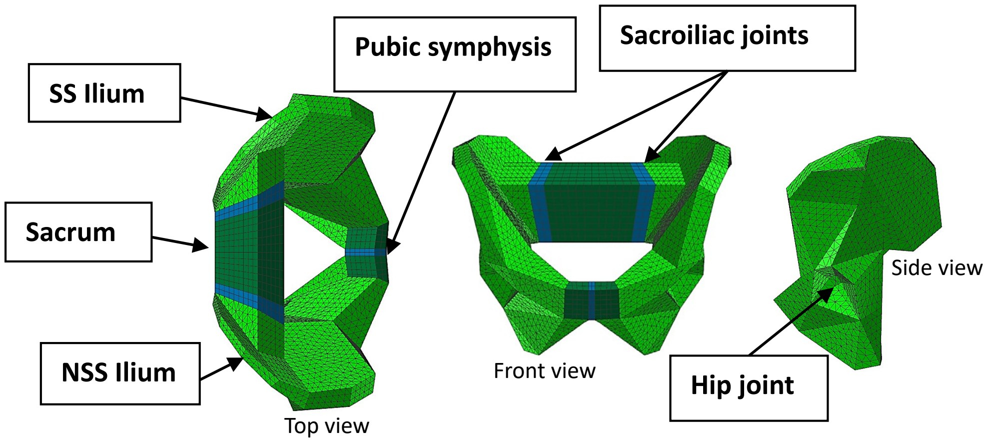

Fig. 24. Isolated views of the simplified pelvis geometry.

Simplification of the Hip Joint and Addition of the Ligaments to Compliant Joints

The hip joint of the reduced HBM was simplified using the same pivot location as the HBM at the acetabulum and spherical joint mechanism (Fig. 25). For simplification, the ligaments surrounding the hip joint modelled in the full-scale HBM were removed and a spherical joint element was defined between the femoral head of the reduced HBM and the acetabulum of the modified pelvis model. Results from a previous study suggested that the pelvis response correlation to HBM greatly improves when the location of this mass is offset laterally by 100 mm from its original position of the NSS acetabulum reference point [21]. Therefore, the previously mentioned 3.87 kg nodal mass was added to the NSS ilium at 100 mm offset from the NSS acetabulum, using nodal rigid body (RB) definition.

When the ligaments surrounding the sacroiliac joint and pubic symphysis generate tensile force, the force is added to the compressive force at the joint surface, causing a higher load at the joint surfaces and a higher risk of fracture. Previous research found that with the definition of wire cables surrounding these joints, this mechanism was found to be physically represented [20]. Based upon this, a series of steel cables were also defined within the pelvis FE model to improve correlation of compressive force responses with the full-body HBM. Initially, four ligament elements were assigned to each joint. These elements were modelled as 5 mm diameter beam elements, aiming to generate no resistance in compression (Fig. 26). The sacroiliac ligament elements were rigidly attached to the ilium and sacrum on their end nodes, while the public ligament elements were rigidly connected to the SS ilium and NSS ilium on their end nodes.

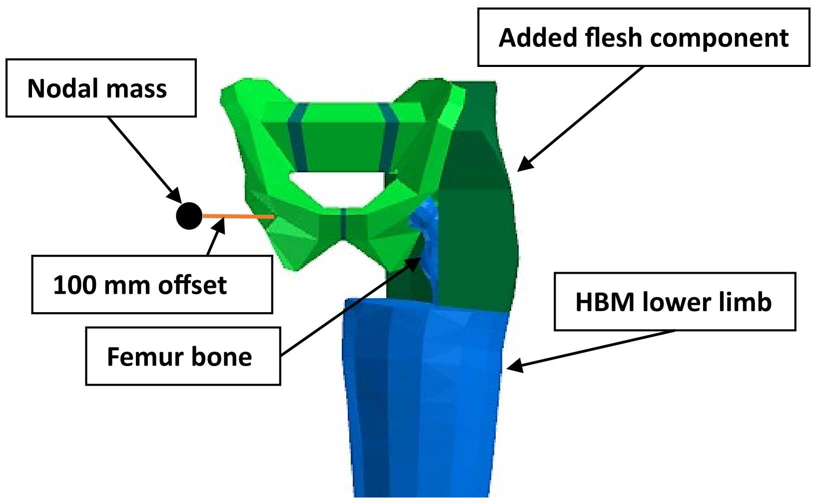

Fig. 25. Simplified NSS LL representation of the reduced HBM.

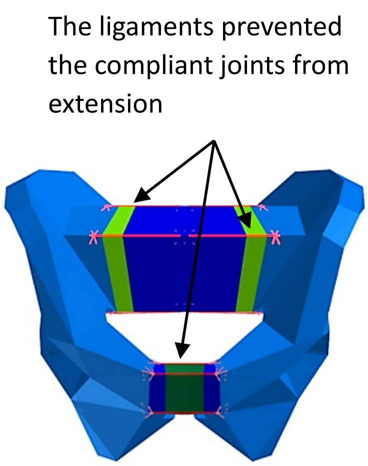

Fig. 26. Four ligaments assigned to each compliant joint.

Allocation of the Initial Materials to the Simplified Pelvis Model

With the initial geometry defined, the material selection process was initiated with the focus on sourcing appropriate materials with similar mass to the corresponding HBM pelvis components. The initial list of materials and a comparison of the component mass is shown in TABLE II.

TABLE II
THE INITIAL LIST OF THE ASSIGNED MATERIAL TO THE SIMPLIFIED PELVIS MODEL AND A COMPARISON OF THE COMPONENT MASS BETWEEN THE SIMPLIFIED PELVIS MODEL AND THE FULL-BODY HBM PELVIS.

Component	Initial Material	Mass in Simplified Pelvis Model (g)	Mass in Full-Body HBM (g)	Difference (%)
Iliac wing (SS and NSS)	Nylon	457	346	32
Sacrum	Aluminium	329	211	56
Pubic symphysis	PU 70A	11	9	22
Sacroiliac joint	PU 80A	24	25	4
Hip flesh	PU 50A	1804	1768	2

The mass of the nylon iliac wing was higher compared to the full-body HBM due to its higher density and volume. The sensitivity study (TABLE I) highlights that the stiffness of the NSS iliac wing has an influence over the pelvis deflection response. However, it was necessary to introduce a material which can withstand the applied stresses without plastic deformation. The sacrum component mass was also 56% higher than the HBM's sacrum, however, the results in TABLE I show that the pelvis injury metrics were not sensitive to the sacrum attributes. The criterion for selecting the initial materials for the compliant joint was the stiffness of the material to represent a close structural stiffness compared to the compliant joint of the full-body HBM. The choice of the material for the hip flesh was based on the stiffness and density compared to the full-body HBM LL flesh characteristics. During this preliminary phase, the sacroiliac joint and pubic symphysis materials had a reduced stiffness compared to those of the full-body HBM to compensate for the stiffer iliac wing material.

Simplifying the Hip Joint Degrees of Freedom

Next step of the simplification focused on the behaviour of the hip joint, where two scenarios were assessed. In scenario 1, a spherical joint was defined at the hip joint and all the rotational degrees of freedom (DOF) were released. In scenario 2, the only released DOF was the rotation about the y-axis (Fig. 27). Both cases were subjected to Sedan, SUV-Low and SUV-High loading conditions. A single axis joint would be more feasible for a physical UM as it would incur less maintenance and variability. Furthermore, a single axis joint represents what is currently defined within the aPLI to connect the UM to the LL. As the aim of the modified UM is to develop a device which can integrate directly into the aPLI LL, therefore, this joint constraint should also remain consistent.

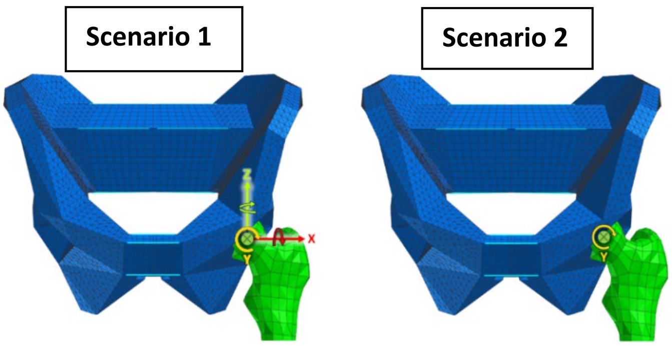

Fig. 27. Hip joint degrees of freedom. Scenario 1: a free spherical joint, Scenario 2: a spherical joint with only free rotation about the y-axis and rotation about x- and z-axis rigidly constrained.

Despite all those considerations, different options must have been investigated to make sure that the injury assessment capability of the simplified pelvis model fall within the acceptance criteria.

Fig. 28 compares the pelvis responses between the two scenarios. The results show only minor differences between the two scenarios for the pelvis displacement, pubic symphysis force and sacroiliac joint force, particularly within the first 30 ms where the peak values of these injury metrics are taken.

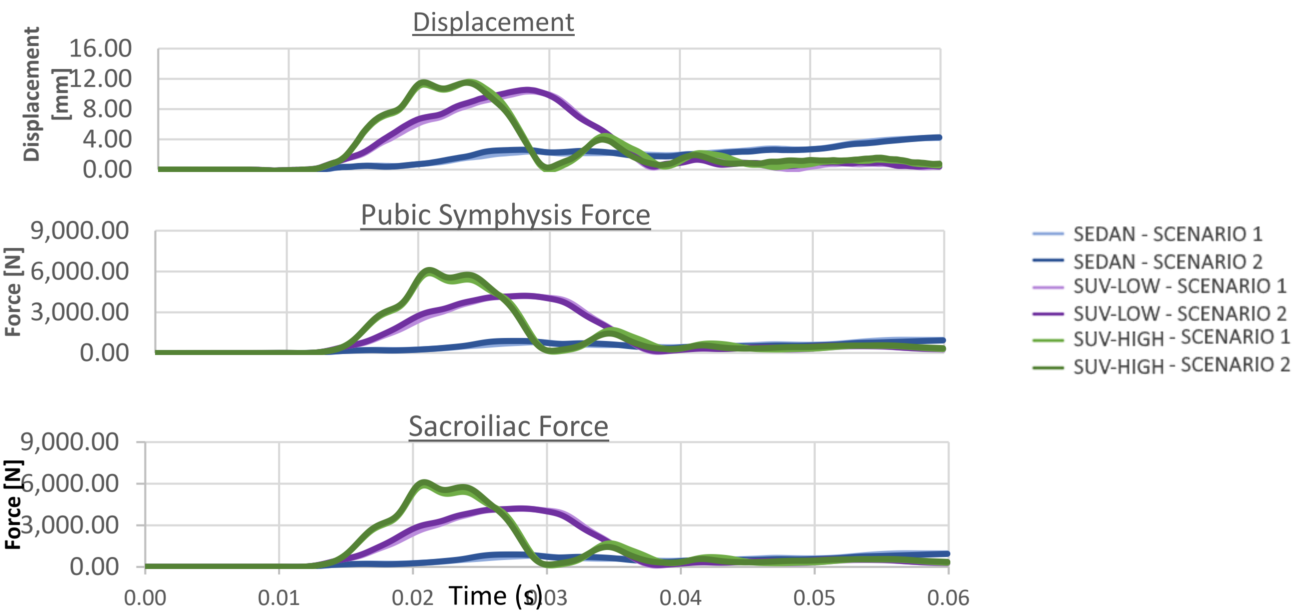

Fig. 28. Comparison of the pelvis responses between Scenario 1 and 2.

Step 3: Modifying the Position of the Concentrated Mass on the NSS Acetabulum

A concentrated nodal mass of 3.87 kg was defined within the preliminary pelvis model at the NSS acetabulum. This nodal mass is a component which can only be represented with the FE model and could not be represented physically. A sensitivity study was performed to assess the influence of the nodal mass vertical position on the pelvis responses. The pelvis model parameters other than the location of the concentrated nodal mass remained consistent in the sensitivity study. The nodal position was incrementally changed in the vertical direction by + 20 mm and + 40 mm to assess potential influence (Fig. 29). The models were subjected to the Sedan, SUV-Low and SUV-High impacts at 11.1 m/s.

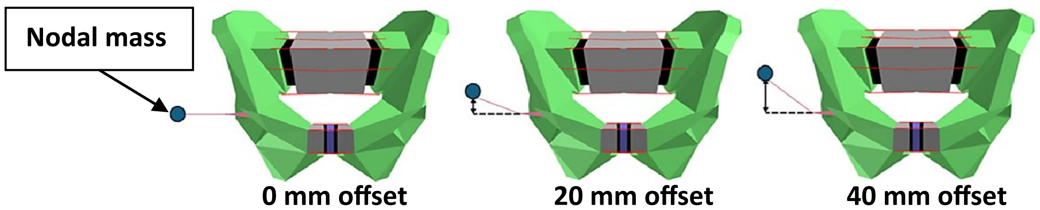

Fig. 29. Simplified pelvis models for a sensitivity study with regard to the vertical location of the concentrated nodal mass on the NSS acetabulum.

Fig. 30 shows the responses of the simplified pelvis model compared to the baseline HBM responses when the position of the nodal mass at the NSS acetabulum was incrementally changed vertically. The pelvis displacement for the Sedan SCM was not influenced notably, however, in the SUV-Low and SUV-High SCM impacts, the displacement was marginally reduced as the nodal position increased in the vertical axis. The sacroiliac joint force from the Sedan SCM had the largest variance, however, there appears to be no significant correlation between the nodal position and the force. A significant variance of the pubic symphysis force was present only in impacts against the SUV-Low and SUV-High SCMs.

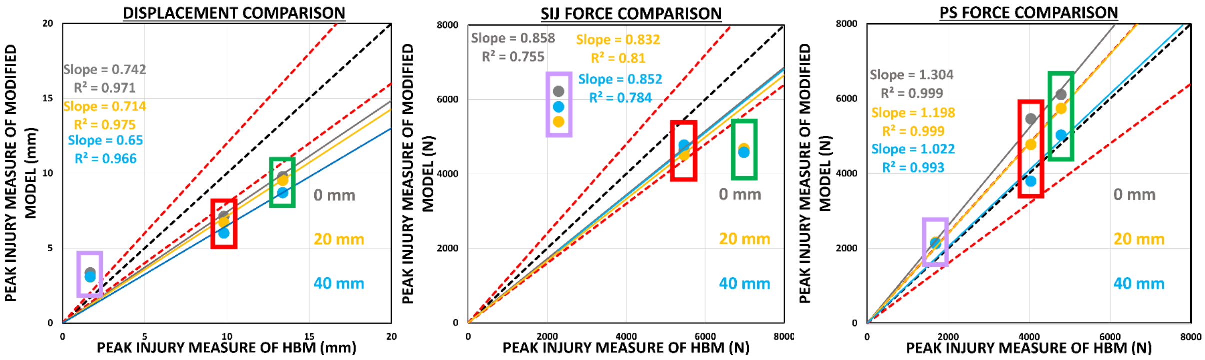

Fig. 30. Responses of the simplified pelvis model compared with the baseline HBM when the nodal mass position is varied vertically.

Step 4: Parametric Study of the Effect of Material variation on Pelvis Injury Metrics

Materials were provisionally assigned to the pelvis component of the reduced HBM at the beginning of this study. However, the influence of the changes in the material type on the pelvis injury metrics was studied to ensure pelvic injury assessment capability of the simplified pelvis model. A parametric study was carried out by assigning several candidate materials to each component individually from other components. Specific candidate materials were chosen based on the mass and the stiffness. Clearly, in a process of a reasonable variation, the component mass would contribute to the pelvis's inertial response, while the stiffness of the parts would affect the pelvis deflection. TABLE III shows a summary of the candidate materials for each component and the reasoning for the selections.

TABLE III
CRITERIA TO CANDIDATE SPECIFIC MATERIAL LIST FOR EACH COMPONENT DURING THE PARAMETRIC STUDY

Component	**Material 1**	**Material 2**	**Material 3**	**Reason for choice**
Ilium (SS/NSS) 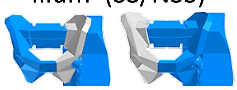	Nylon	Aluminium	Steel	Reasonable balance between stiffness and inertial behaviour
Sacrum 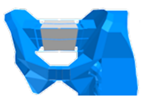	Nylon	Aluminium	N/A	
Hip flesh 	Polyurethane-30A	Polyurethane-50A	Polyurethane-60A	Improved compliant joint loading response through the elastic deformation
Sacroiliac joint 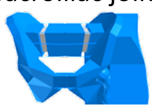	Polyurethane-50A	Polyurethane-60A	Polyurethane-80A	Reasonable stiffness response
Pubic symphysis 	Polyurethane-50A	Polyurethane-60A	Polyurethane-70A	

During this parametric study, each iteration model was subjected to the Sedan, SUV-Low and SUV-High impact at 11.1 m/s and the results were recorded individually. The final choice of the material was based the most optimum pelvis response compared with the baseline HBM responses.

Fig. 31 shows the responses of the simplified pelvis model compared to the baseline HBM responses when nylon, aluminium and steel materials were assigned to the SS ilium. It was expected that by increasing the stiffness of the material, the pelvis deflection would reduce. This reduction incurred a negative effect on the correlation of the pelvis deflection when compared to the baseline HBM. There appeared to be no significant positive influence when the stiffer materials were implemented. Therefore, the nylon material remained unchanged in the SS ilium component.

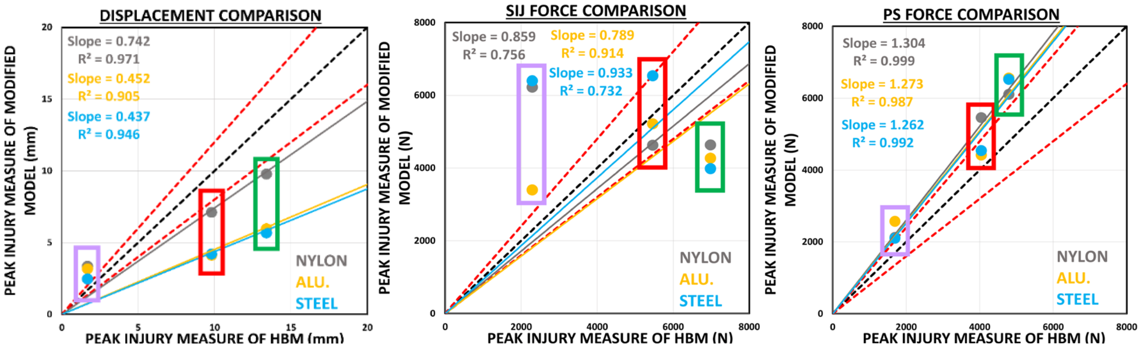

Fig. 31. Pelvis responses of the simplified pelvis model compared with the baseline HBM responses when the material type is varied in the SS ilium.

Fig. 32 shows the responses of the simplified pelvis model compared to the baseline HBM responses when nylon, aluminium and steel materials were assigned to the NSS ilium. The results show that the pelvis deflection was reduced for the denser materials. This negatively affected the correlation to the baseline HBM responses. The sacroiliac joint force correlation was improved insignificantly for the SUV-Low and SUV-High SCM simulations, whereas the pubic symphysis force correlation was reduced marginally for the denser materials. Therefore, the material was changed to steel to not only aid with achieving the assembly mass but also to help with maintaining the behavioural kinematics of the simplified pelvis model.

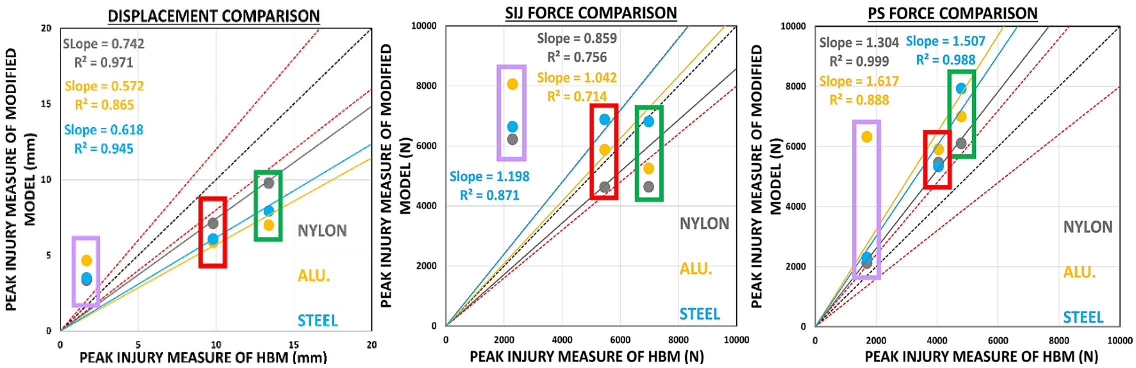

Fig. 32. Pelvis responses of the simplified pelvis model compared with the baseline HBM responses when the material type is varied in the NSS ilium.

Fig. 33 shows the responses of the simplified pelvis model compared to the baseline HBM responses when nylon and aluminium were assigned to the sacrum. The results show that for both displacement and pubic symphysis force responses, the correlation did not change significantly between both material models. A reduction was observed for the sacroiliac force when compared with the baseline HBM response. Since the correlation of the peak values of the pelvis injury metrics did not offer a significant evidence to select a better material for this component, the time history plots of those metrics were compared to the baseline HBM model specifically for the Sedan impact as shown in Fig. 34. In case of the aluminium material, a significant difference was observed in the Sedan SCM simulation for the pelvis displacement and sacroiliac joint force where their maximum values were reached in a later stage of the simulation compared to the baseline HBM response. Nylon material offered a better correlation to the baseline HBM in the Sedan SCM simulation, therefore the material was changed to Nylon in this component.

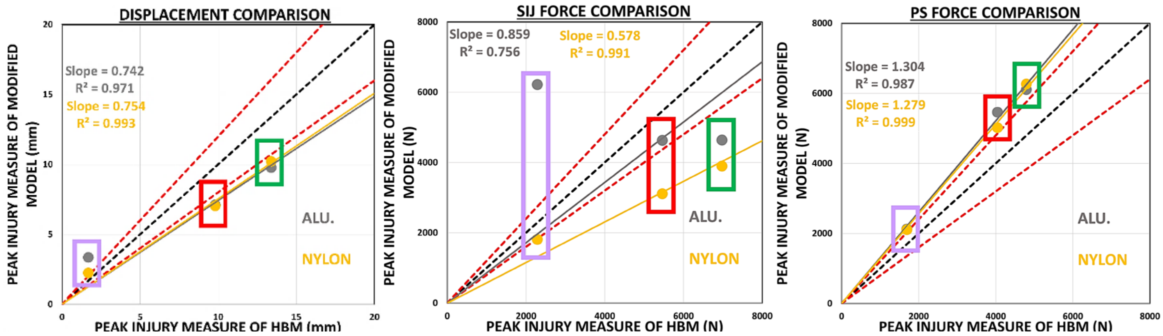

Fig. 33. Pelvis responses of the simplified pelvis model compared with the baseline HBM responses when the material type is varied in the sacrum.

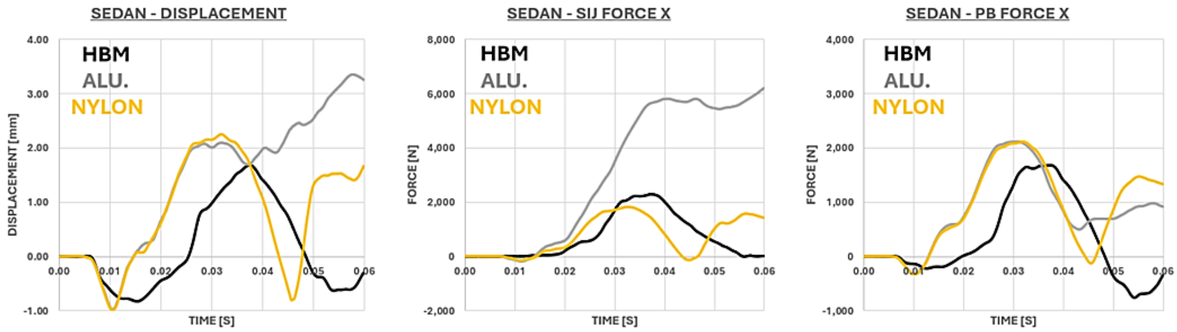

Fig. 34. Time history plots of the pelvis injury metrics compared with those of the baseline HBM when the material type is varied in pubic symphysis in Sedan SCM impact.

Fig. 35 shows the responses of the simplified pelvis model compared to the baseline HBM responses when PU 30A, PU 50A and PU 60A were applied to the hip flesh. These results indicated that the pubic symphysis force responded better for the 30A material in comparison to the harder materials. There was also an improvement in the correlation for the sacroiliac force in the Sedan load case with the maximum value reducing as the hardness of the material reduces. There was not a large influence in the material for the deflection response, which was contrary to the influence expected to be seen based upon the sensitivity analysis conducted upon the baseline HBM. Based upon the influence observed, a 30A material was selected for the best correlation with the baseline HBM responses.

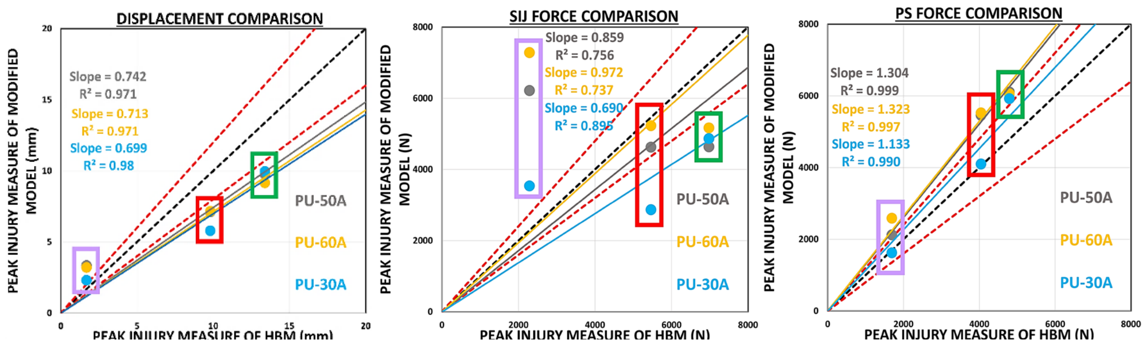

Fig. 35. The simplified pelvis model responses compared to the baseline HBM responses when the material type is varied in the hip flesh.

Fig. 36 shows the responses of the simplified pelvis model compared to the baseline HBM responses when PU 50A, PU 60A and PU 80A were assigned to the cartilage at the sacroiliac joint. The findings showed that there was a significant influence in the deflection response when the stiffness was reduced. The deflection increased as the stiffness is reduced. Based upon the deflection results, both the 60A and 50A materials had a good correlation to the baseline HBM response. The pubic symphysis force comparison showed that the change of materials had no significant difference in this response. The sacroiliac force response showed that the softer materials decrease the maximum value for the Sedan SCM impact. This relationship between the response and the material did not appear to be a linear relationship and there was no significant change in the overall trendline between the three materials tested. Due to the improvement in the correlation of the pelvis deflection, the 50A material was selected as it provides the best correlation overall.

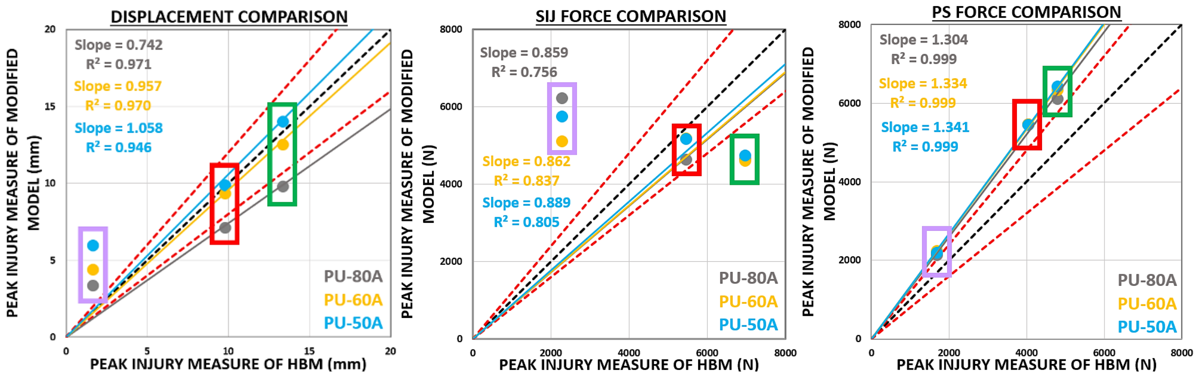

Fig. 36. Pelvis responses of the simplified pelvis model compared with the baseline HBM responses when the material type is varied in the cartilage of the sacroiliac joint.

Fig. 37 shows the responses of the simplified pelvis model compared to the baseline HBM responses when PU 50A, PU 60A and PU 70A were assigned to the cartilage at the pubic symphysis. The results showed no significant influence of the material for this component across all pelvis responses in general. Due to no significant influence being present for these selected materials, the material defined for this pubic symphysis component remains as polyurethane 70A.

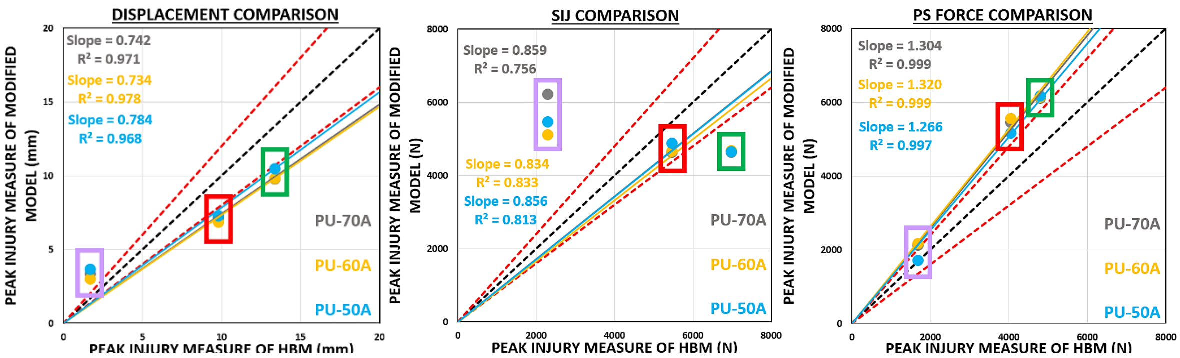

Fig. 37. Pelvis responses of the simplified pelvis model compared with the baseline HBM responses when the material type is varied in the cartilage of the pubic symphysis.

Fig. 38 shows the pelvis responses of the simplified pelvis model when all the components are updated with the finalised materials specified by this parametric study. Comparisons were made against the final model in Step 3. The deflection response was found to be greatly improved to better match the baseline HBM response. In the Sedan SCM impact, the force response correlated well with the baseline HBM response and falls within the tolerance corridor. The sacroiliac force in the SUV-Low impact was lower than that of the baseline HBM, however, they better correlates in the SUV-High impact. The pubic symphysis response correlated closely with the baseline HBM in the SUV-Low impact, however, the maximum force in the SUV-High SCM impact was higher than that of the baseline HBM. This higher force could be attributed to the influence of the NSS steel iliac wing which showed a high pubic symphysis force for the SUV-High SCM.

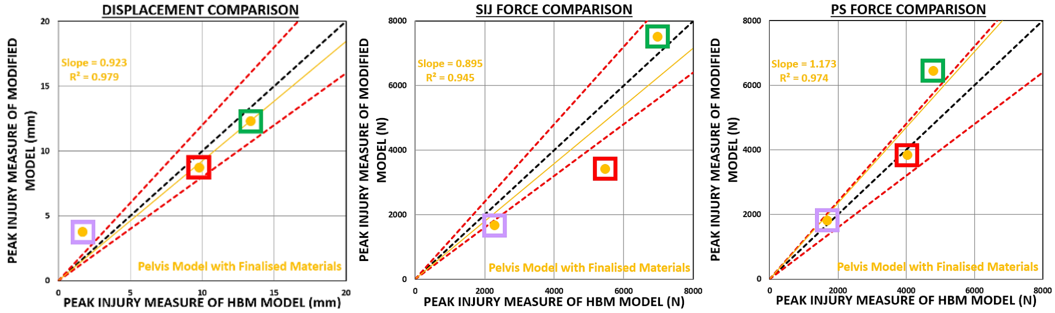

Fig. 38. Pelvis responses of the simplified pelvis model compared with the baseline HBM responses when the finalised materials are applied to all the pelvis components investigated.

Step 5: Further Simplification of the Insensitive Geometric Attributes

This step of the study aimed to replicate the correlation achieved in the previous step, while defining manufacturable SS and NSS iliac wing component. Simplification of the geometry of the SS ilium and NSS ilium were carried out individually from other components. The unchanged components followed the attributes as defined in Step 4 of this parametric study.

Based on the results summarised in TABLE I, the pelvis responses were sensitive to the mass (hence the CoG) of the NSS ilium, while they were not sensitive to the geometry of this component. Therefore, while the geometry was deemed as changeable, the mass and the CoG of the NSS ilium needed to be maintained. Meanwhile, the nodal mass attached to the NSS ilium is unable to be represented in a physical device and needed to be embedded to this component in a practicable manner. Based on these constraints, several iterative designs were examined to reach a practically manufacturable design for the NSS ilium that also met the pelvis response requirements. Fig. 39 shows the details of the simplified design for the NSS ilium. The steel forms the main structure in this component and a tungsten ballast has been added to surface of the iliac wing to not only reach the target mass for this component, but also to help maintaining the CoG location of the component. The model was subjected to the Sedan, SUV-Low and SUV-High impacts at 11.1 m/s.

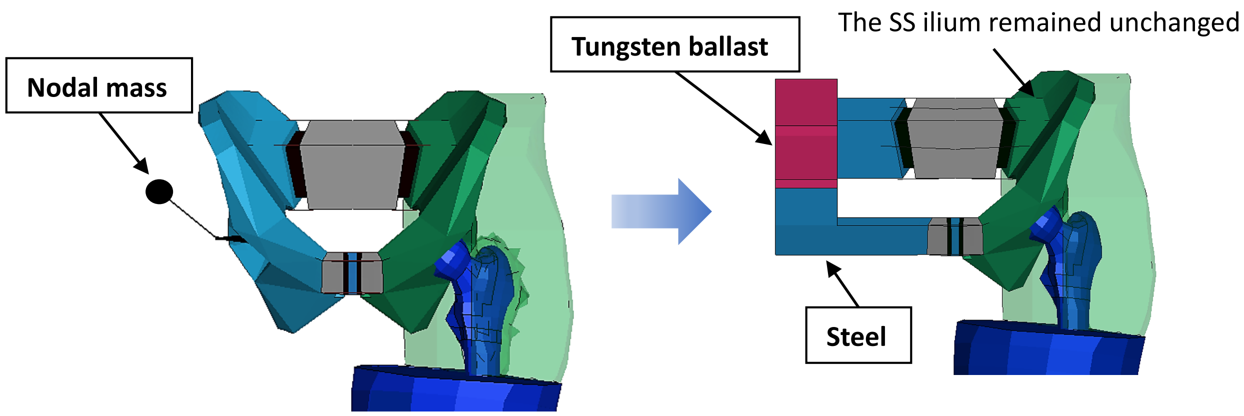

Fig. 39. Simplification of the geometry of the NSS ilium. The nodal mass has been embedded to the main structure and a tungsten ballast has been added to maintain the target mass and CoG location. The SS ilium remained unchanged, while the geometry of the NSS ilium was simplified.

Fig. 40 shows the pelvis responses of the simplified pelvis model compared to the baseline HBM responses when the geometry of the NSS ilium has been simplified. The pelvis response was shown to be highly comparable to the results obtained from Step 4 of this parametric study. With marginal variation in responses, the response tolerance criteria remained very close.

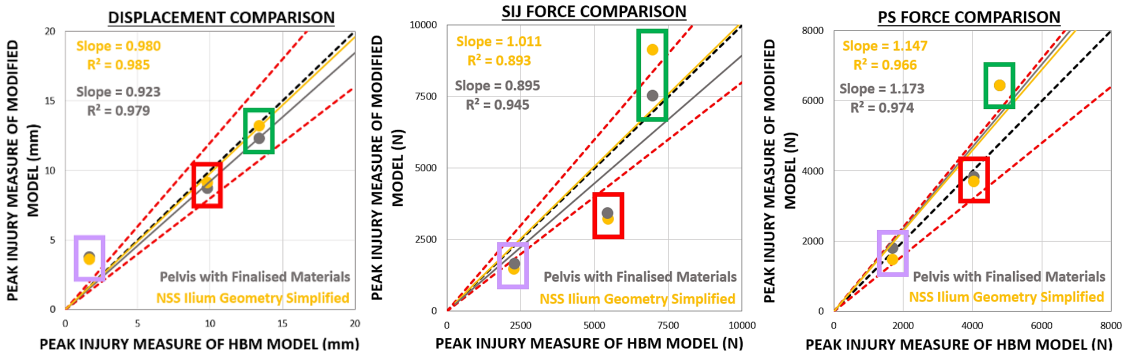

Fig. 40. Pelvis responses of the simplified pelvis model compared with the baseline HBM responses when the geometry of the NSS ilium has been simplified.

Although the results in TABLE I suggested that the pelvis responses were sensitive to the geometry of the SS ilium, for ease of manufacturing, it was necessary to simplify this component. Nonetheless, the upper section of the iliac wing and the hip joint remained unchanged and biofidelic in shape to ensure that the SCM-pelvis contact timings remained consistent with the baseline HBM, while simplifying the design. Fig. 41 shows the details of the SS ilium with a simplified geometry. During this process, the geometry of the NSS ilium remained unchanged and its attributes corresponded to those determined in Step 4 of this parametric study.

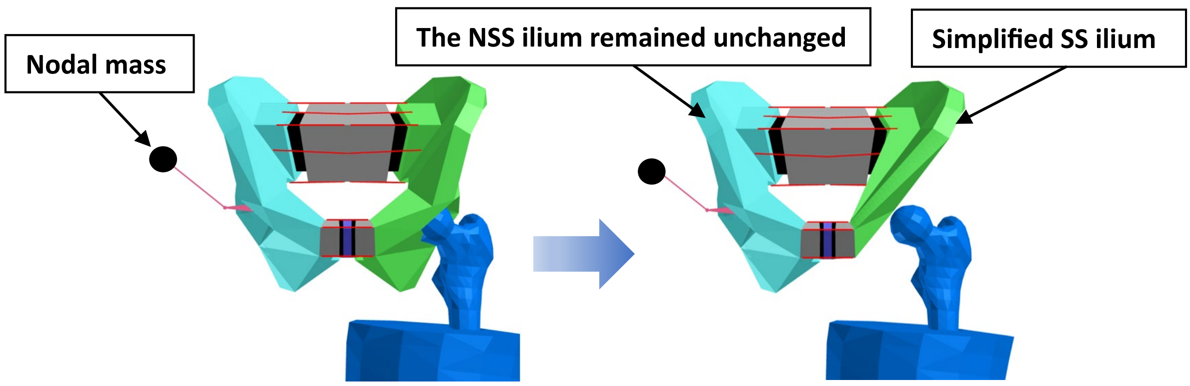

Fig. 41. Simplification of the geometry of the SS ilium. The contact surface of the SS ilium and the hip joint area remained intact. During this process, the attributes of the NSS ilium remained unchanged.

Fig. 42. shows the pelvis responses of the simplified pelvis model compared with the baseline HBM responses when the geometry of the SS ilium has been simplified. The simplification of the insensitive geometry of the SS ilium had a minimal influence on the simplified pelvis model responses when compared to the responses from the final pelvis model in Step 4. The pelvis deflection showed the largest difference in results, however, the pubic symphysis and sacroiliac joint force responses showed a relatively close correlation.

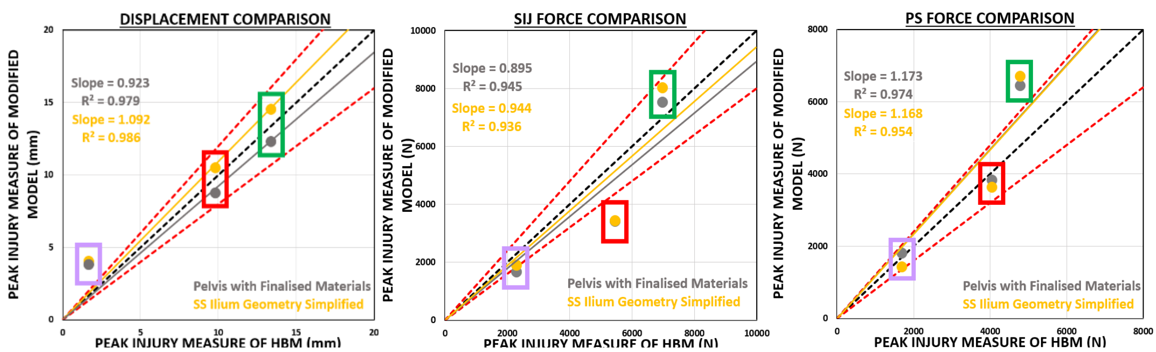

Fig. 42. Pelvis responses of the simplified pelvis model compared with the baseline HBM responses when the geometry of the SS ilium has been simplified.

The final model for the reduced HBM contained the simplified hip joint model, selected materials for the pelvis components and the simplified geometries for the SS and NSS ilium parts. the simplified SS and NSS ilium were combined to form a reduced HBM with the simplified pelvis model that offers design parameters of a functioning prototype for a modified UM (Fig. 43).

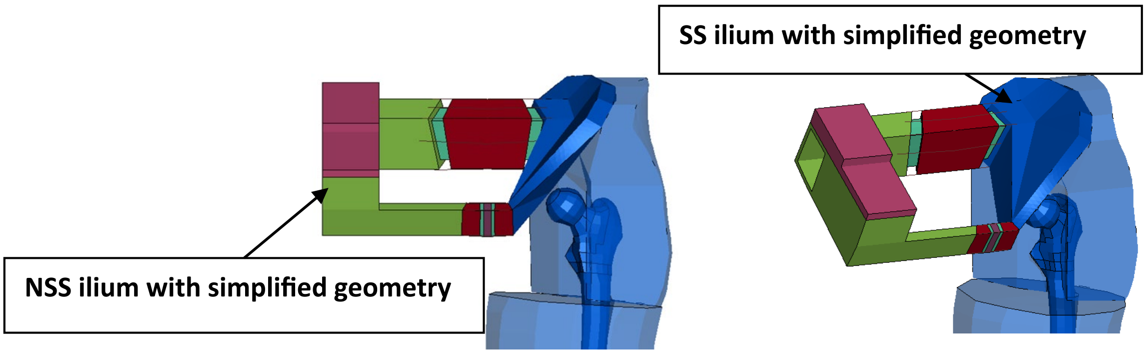

Fig. 43. The final simplified pelvis model of the reduced HBM.

Fig. 44 shows the pelvis response in the reduced HBM when the model is first updated with the selected materials for the components and then additionally with the simplified geometries of the SS and NSS ilium.

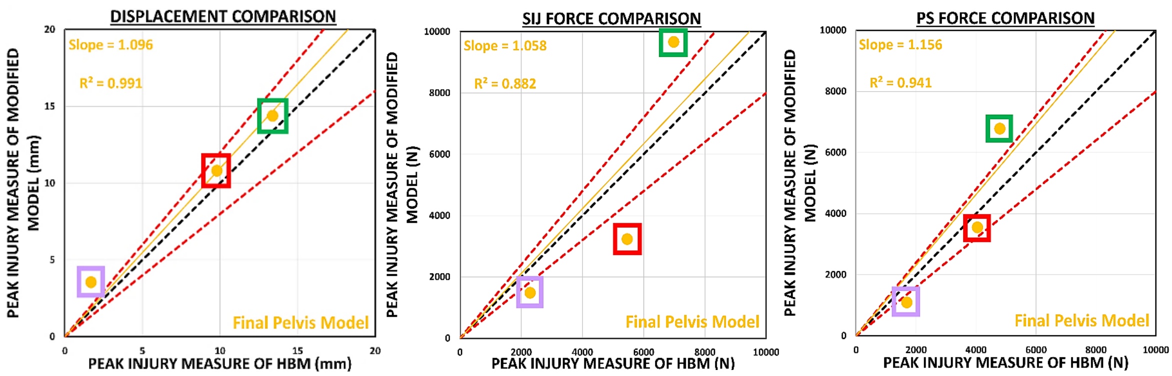

Fig. 44. Pelvis responses of the final simplified pelvis model of the reduced HBM compared with the baseline HBM responses.

APPENDIX 2: COMPARISON OF THE PHYSICAL PROPERTIES OF THE PRTOTYPE-1 UM COMPONENTS WITH THE SIMPLIFIED PELVIS MODEL OF THE REDUCED HBM

Note: *The centre point of rotation for the hip joint was used as the reference point for the dimensions shown in the following tables in both the simplified pelvis model and prototype-1. Fig. 45 Shows the direction of the axis at the centre point.*

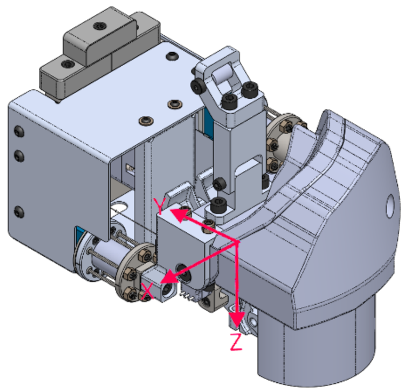

Fig. 45. Direction of the X, Y and Z axis at the centre point.

TABLE IV

COMPARISON OF MASS AND COG LOCATIONS OF THE SS ILIUM

	Simplified Pelvis Model	Prototype-1	Difference (%)
Mass (kg)	0.4	0.5	26
X (mm)	-19.4	-20.5	6
Y (mm)	-27.0	-29.7	10
Z (mm)	-45.7	-50.8	11

TABLE V

COMPARISON OF THE MOMENT OF INERTIA ABOUT THE COG OF THE SS ILIUM

	Simplified Pelvis Model ($kg.mm^2$)	Prototype-1 ($kg.mm^2$)	Difference (%)
Ixx	618.6	685.7	11
Ixy	10.6	21.3	101
Ixz	181.1	193.2	7
Iyy	831.0	1188.2	43
Iyz	223.3	242.3	9
Izz	614.3	1082.2	76

TABLE VI

COMPARISON OF MASS AND COG LOCATIONS OF THE COMBINATION OF THE SACRUM, SACROILIAC JOINT AND NSS ILIUM

	Simplified Pelvis Model	Prototype-1	Difference (%)
Mass (kg)	7.26	7.1	2
X (mm)	-11.1	-8.2	25
Y (mm)	162.8	167.2	3
Z (mm)	-38.4	-37.8	1

TABLE VII

COMPARISON OF THE MOMENT OF INERTIA ABOUT THE COG OF THE COMBINATION OF THE SACRUM, SACROILIAC JOINT AND NSS ILIUM

	Simplified Pelvis Model (kg.mm²)	Prototype-1 (kg.mm²)	Difference (%)
Ixx	18582.7	21953.2	18
Ixy	3444.7	462.3	87
Ixz	5619.9	2567.5	54
Iyy	26403.2	31123.1	18
Iyz	416.4	632.5	52
Izz	19667.4	18787.4	4

TABLE VIII

COMPARISON OF MASS AND COG LOCATIONS OF THE HIP FLESH

	Simplified Pelvis Model	Prototype-1	Difference (%)
Mass (kg)	1.8	1.2	33
X (mm)	-41.6	-15.0	64
Y (mm)	-77.4	-88.2	14
Z (mm)	3.7	-39.4	1168

TABLE IX

COMPARISON OF THE MOMENT OF INERTIA ABOUT THE COG OF THE HIP FLESH

	Simplified Pelvis Model (kg.mm^2)	Prototype-1 (kg.mm^2)	Difference (%)
Ixx	7786.9	2241.2	71
Ixy	945.2	235.6	75
Ixz	156.4	558.6	257
Iyy	7993.0	3246.4	59
Iyz	59.4	136.7	130
Izz	3299.2	2522.8	24

TABLE X

COMPARISON OF THE GEOMETRIC PARAMETERS OF THE COMPLIANT JOINT

	Simplified Pelvis Model		Prototype-1		Difference (%)	
	SIJ	PS	SIJ	PS	SIJ	PS
Cross-section [mm^2]	1082.0	481.8	615.8	615.8	43	28
Depth [mm]	22.9	14.6	40.0	40.0	75	174